

CERN Beam Test of Silicon-Tungsten Calorimeter Test Module

S.Nam, J.Lee, I.H.Park, H.J.Hyun, J.Yang
Ewha Womans University, Seoul, 120-750, Korea
J.H.Choi, J.S.Kang, S.K.Park
Korea University, Seoul, 136-701, Korea
B.S.Jang, S.H.Jeong, J.H.Kang, Y.J.Kwon
Yonsei University, Seoul, 120-749, Korea
I.T.Yu, Y.P.Yu
Sungkyunkwan University, Suwon, 440-746, Korea
Y.D.Oh
Kyungpook National University, Daegu, 702-701, Korea

PIN diode silicon sensors with low leakage current were developed as 4×4 pixel arrays from 5 inch wafers. A test module of silicon-tungsten calorimeter was designed, built using the sensors, and tested with high energy beam of electron, muon, and hadrons for the study of its application at the future linear collider. The construction of the test module and the results of the beam test are discussed.

1. INTRODUCTION

The silicon-tungsten calorimeter has been proposed as an electromagnetic calorimeter at the future linear collider experiment [1]. This detector can be constructed in a fine granularity and in a small effective Moliere radius so that single particle showers produced in a jet of linear collider events could be resolved individually. It has been shown that this detailed jet reconstruction results in a high jet energy resolution when combined with tracking information [2]. One of challenges in building the calorimeter is in producing large amount of high quality silicon sensors with an uniform characteristics.

Our effort has been on the sensor R&D for the high yield production of low noise sensors. This talks describes the beam test of a small test calorimeter built using the sensors we developed as pixel arrays.

2. CONSTRUCTION OF TEST MODULE

2.1. Silicon Sensors

A silicon sensors is a 4×4 array of 16 PIN diode pixels. The beginning of the sensor is 5 inch single-sided polished wafer with $380 \mu\text{m}$ thickness. The wafers were delivered with $15 \mu\text{m}$ thickness variation in wafer to wafer RMS and less than $3.5 \mu\text{m}$ in the variation within a wafer. The bulk resistivity of the wafer is bigger than $5 \text{ k}\Omega\text{cm}$. The process of optimizing parameters in the fabrication procedure was performed with mask patterns containing three guard rings around the array [3]. The size of a sensor is $6.52 \times 5.82 \text{ cm}^2$ with a pixel size of $1.55 \times 1.37 \text{ cm}^2$. The post-fabrication procedure for sensor packing is described in Figure 1.

Various tests during the fabrication and packing processes were taken to measure the characteristics of individual pixels. First, the sensor capacitance was measured as the bias was gradually increased. The full depletion of sensors are established at around 90V for the most of sensors and the depletion state stays stable up to few hundreds volt. In order to make sure all sensors operate at the full depletion 100V was applied as a practical bias voltage, considering the variation in the sensor thickness and the wafer resistivity. Leakage current was measured for all pixels. Figure 2 shows the leakage current for pixels of a typical sensor. Most pixels have the leakage current level below 10nA at

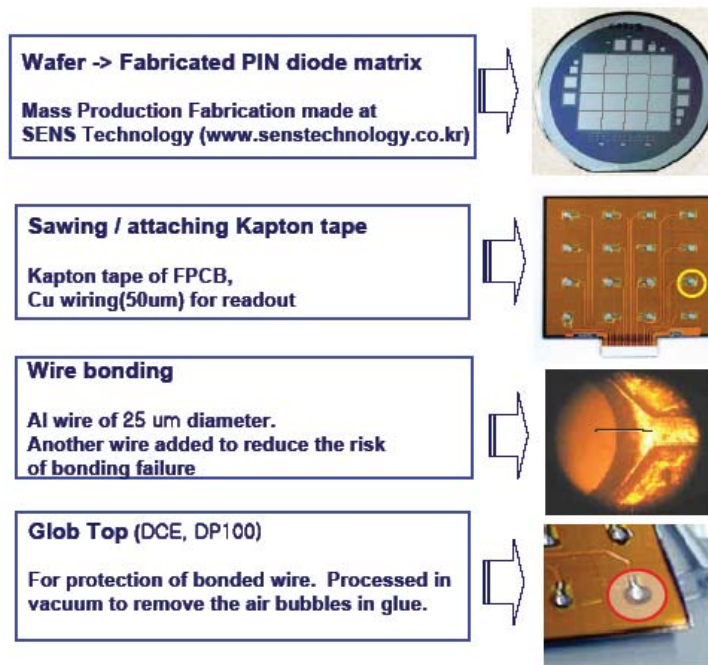


Figure 1: The post-fabrication packing process for a silicon sensor.

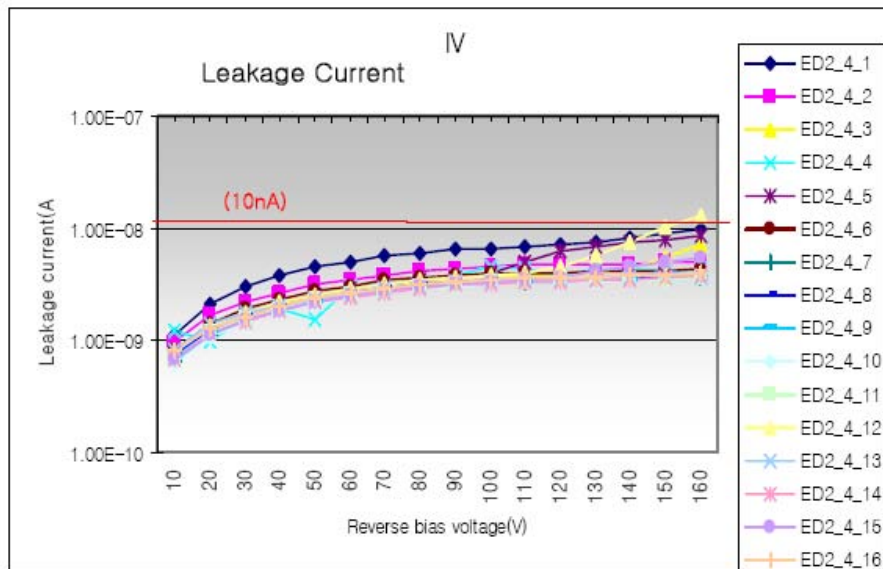


Figure 2: Leakage current measurement of 16 channels in a sensor as a function of bias voltage. The operational bias level applied for full depletion is 100V.

the bias of full depletion. With the quality condition that all the pixels in a sensor should have the leakage current below 20nA at the full depletion, the sensor yield in the optimized production is close to 90% when estimated after the final packing process. The test with radioactive source of Sr-90 was also performed and the clean signal was seen to be nicely fitted to a Landau distribution.

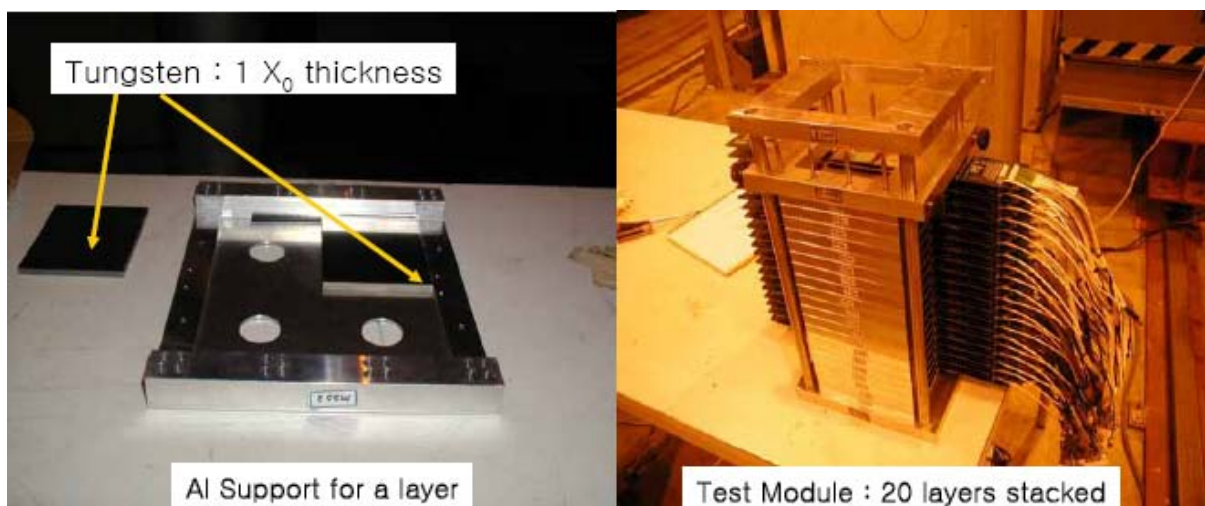


Figure 3: (Left) Aluminum support for a calorimeter layer and Tungsten pieces. (Right) Assembled test module with frontend boards, stacked in 20 layers. Two sensors were installed in a layer.

2.2. The Frontend Electronics and Mechanics

The frontend electronics was built around CR1.4 chips that had been designed for a cosmic ray measurement [4]. A CR1.4 chip handles signals from 16 pixels of a sensor and the charge inputs are converted to a multiplexed sequence of held-DC levels of the channels. The wide dynamic range of the chip allows to cover up to the signal of 1400 MIPs in a channel. 16bit ADCs were used allowing digitization precision fine enough for our test. The data acquisition system was set up using electronics available from our previous project. During the beam test operation, 10% out of 640 readout channels were found to be too noisy to identify MIP signals. Another 10% of channels suffered from unstable functioning of ADC chips. In addition, there were dead channels of about 2%.

Tungsten pieces were prepared in the thickness of one radiation length $1 X_0$ (3.5mm) for all layers. Aluminum structure were prepared to support 20 layers of tungsten, frontend boards, and silicon sensors. A layer consists of two sensors that were arranged to have 1mm insensitive gap between sensors because of the insensitive sensor edges. The total thickness of a layer is 15mm including aluminum plate of the support mechanics. The effective Moliere radius of this composite system is 45mm.

In summary, the test module is 20 layers of silicon and tungsten sandwiched in an uniform thickness of one radiation length of tungsten. The front of layers is sensors which means the module has 19 actual layers of shower sampling. The area inside a Moliere radius is larger than a sensor size, resulting in insufficient transverse containment of an electromagnetic shower. The loss of shower is also expected in the longitudinal tails from high energy beams. No action were taken for colling the frontend electronics. The assembled detector module is shown in Figure 3.

3. BEAM TEST PROCEDURE

The beam test was carried out at CERN H2 Beam line for a week till September 7th 2004. High energy test beam of electron, muon, and hadrons was served from 10 GeV to 150 GeV. The test module was directly exposed to the beam without tracking system in the front. Three stations of plastic counters in different sizes located about 20m upstream in the beam line were used to monitor the focus state of incident beam. Only coincidences of all three counters produced the trigger signal for the beam events. Trigger was organized in such a way that random triggers were mixed between beam triggered events in order to take the pedestal data for offline analysis.

The detector was installed in a table that was equipped with automated moving machine that allows us to make alignment of the detector along the beam line without interrupting beam. The position of detector was finally aligned

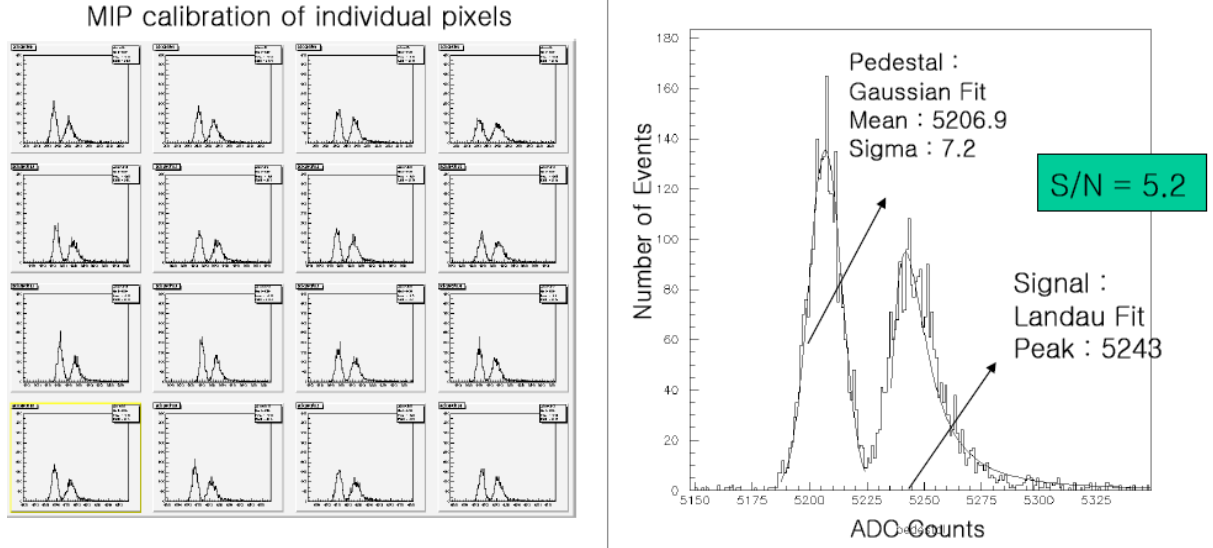


Figure 4: (Left) MIP calibration using 100 GeV hadron beam. (Right) Signal to noise ratio of a typical pixel.

to the beam by monitoring the position of electron shower profile. The data for MIP calibration were then taken by scanning over all channels in a layer with better focused hadron beam. This time, tungsten pieces were removed from all layers during the runs. High energy beam data was taken for muon, hadron, and electron beams with steps of beam energy 10, 20, 30, 50, 80, 100, and 150 GeV. During the period the center of beams were aligned to the the center of one of two sensor in a layer.

4. RESULT OF BEAM TEST

Figure 4 shows the result of MIP calibration for channels in a sensor. The peaks in the left side of plots show pedestal signals from randomly triggered events while the peaks in the right sides are MIP signals produced by the high energy beam. The signal to noise(SN) ratio was measured to be 5.2 from Gaussian fit to the pedestal distribution and Landau fit to the MIP signals. The SN ratio appeared uniform over most of pixels connected to good readout channels.

The detector response to three different type of beam is shown in Figure 5. The pedestal signal from the random trigger events is seen in the peaks of the left side of plots. Total signal from all channels for 50 GeV electron beam is shown in the top plot. When the pixel signals are plotted in the longitudinal arrangement of channels, typical electromagnetic shower profile is clearly visible as shown in the right plot. In the profile plot, the readout pedestals were subtracted. For electron runs the total signal shape above pedestal were fit to a Gaussian distribution. Channel gains were not corrected here yet. The size of total signal is found to be linear over entire range of test beam energy. From the data, the energy resolution to high energy electron was measured to be $28\%/\sqrt{E}$. The MC simulation under the same detector geometry gives $18\%/\sqrt{E}$ for a perfect readout condition. The discrepancy between MC result and beam data is expected to be due to the failure in the part of readout electronics, the spread in test beam, and the variation in readout channel gains. These effect were not taken into account in the MC simulation. The further analysis is on the way to estimate the influence in the simulation.

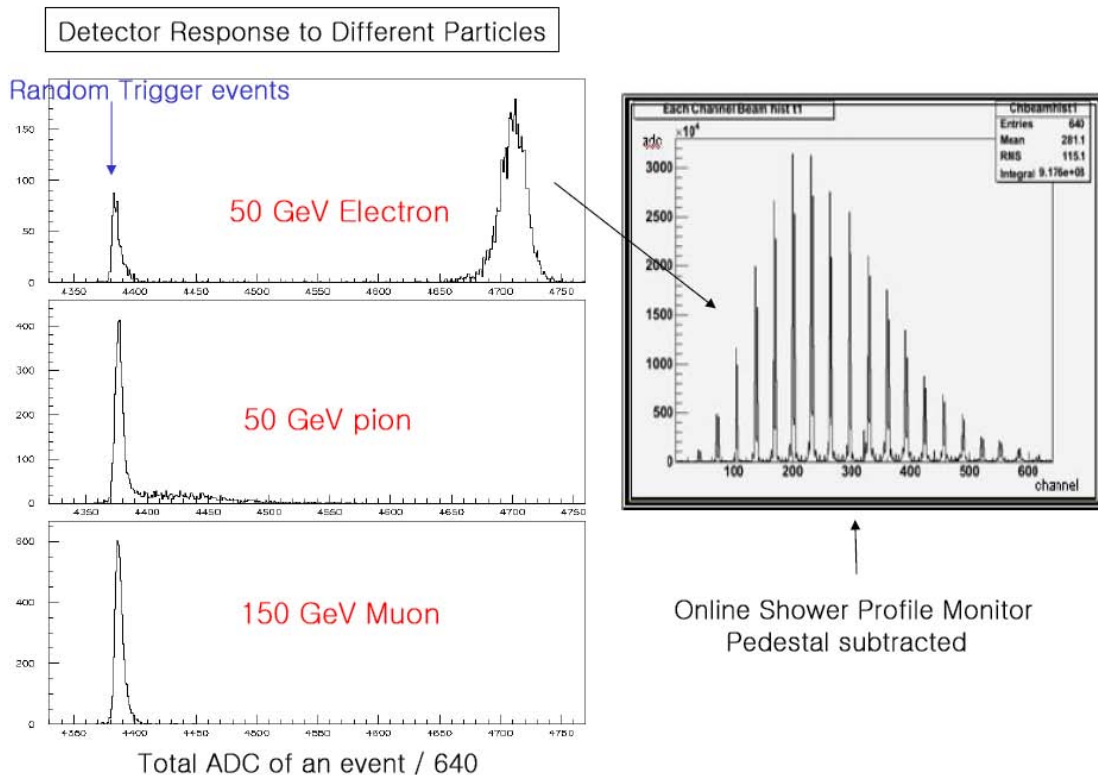


Figure 5: (Left) Detector response to different particles. (Right) Longitudinal shower profile from 50 GeV electron beam.

5. SUMMARY

PIN diode silicon sensors were developed in 4×4 pixel arrays from 5 inch wafer of $380 \mu\text{m}$ thickness. The fabrication condition was successfully optimized for the high yield of good quality sensors that have channel leakage current lower than 20 nA at the full depletion bias. A small test module of silicon-tungsten calorimeter were built using the sensors in 20 layers with $1 X_0$ each layer. The test of the module was performed using high energy beam from 10 GeV to 150 GeV at CERN. The signal-to-noise rate was measured to be 5.2 with readout electronics applied using CR1.4 chips. Typical detector responses and shower profiles to the various type of beam at different energy were obtained.

Acknowledgments

We would like to thank A. Malinine for the beam line operation during our test. This work was supported by the Korea Science and Engineering Foundation grant (M60501000115-05A0200-11510).

References

- [1] TESLA Technical Design Report, DESY Report 2001-011, March 2001.
- [2] <http://polywww.in2p3.fr/flc/justif/justif-granul.html>
- [3] I.H. Park, et al., Nucl. Instr. and Meth. A 535 (2004) 158.
- [4] M. Boezio, et al., Nucl. Instr. and Meth. A 487 (2002) 407.